OPTICAL FIBER SENSORS WITH DISTRIBUTED PARAMETERS BASED ON OPTICAL FIBER REFLECTOMETRY

Branislav KORENKO[1], *Jozef JASENEK*[1], *Jozefa CERVENOVA*[1], *Marek HLAVAC*[1]

[1]Department of Electromagnetic Theory, Faculty of Electrical Engineering and Information Technology, Slovak University of Technology in Bratislava, Ilkovicova 3, Bratislava, Slovakia

branislav.korenko@stuba.sk, jozef.jasenek@stuba.sk, jozka.cervenova@stuba.sk, hlavac.marek@gmail.com

Abstract. *The paper concerns the optical fiber sensors with distributed parameters based on the combination of the polarization optical time domain reflectometry (PO-OTDR) and the photon counting OTDR (PC-OTDR) using standard optical fibers (OF). In the first part a simple introduction into the optical fiber sensors and measurement of the pressure, strain, and torsion is brought. Further the principles of PC-OTDR and PO-OTDR and their application to the realization of optical fiber sensors are briefly explained. The sensor model built on the cascade model of OF is also described. The main part of the paper is a detailed numerical model of OF sensor for the strain distribution measurement. Finally the results of the measured data by the PO-OTDR are analyzed.*

Keywords

Optical fiber, optical fiber sensors with distributed parameters, optical time domain reflectometry (OTDR), photon counting OTDR, polarization OTDR, elastooptical phenomenon.

1. Introduction

Nowadays in the field of optical fiber systems more research concerning optical fiber sensors with distributed parameters is required. Architecture and mechanical design of OF enable its implementation into civil engineering structures, airplanes, turbines and other structures for measurement some physical quantities like pressure, vibration etc. Designing a multidimensional structure with OF sensors provides the possibility to measure mechanical or other physical fields in more dimensional manner. Also real time measurement is possible.

The advantage of using OF sensors with distributed parameters instead of those using conventional methods is that only the access to one end of the fiber is needed and it is also possible to measure more dimensional structure with appropriate space resolution.

The usage of conventional sensors needs to create a complicated monitoring net structure with multiple sensors. The wiring of each sensor requires multiplexing and data processing. From the point of realization it is economically more demanding and also more complicated.

OF sensors can be divided into 2 main types - extrinsic and intrinsic. Extrinsic sensors are characterized with detection outside the fiber structure.

At present time OTDR is used in many fields of OF technology. Except others OTDR methods are suited mainly for uniformity tests of optical traces. The main advantage is their nondestructive character. For these methods the access to only one end of the tested fiber is needed.

2. The Principles of PO-OTDR

The first back-scattering measurement method for investigation of local absorption coefficient in optical fibers was introduced by Jensen and Barnoski [1]. This one-end precise technique can be modified by the use of polarization analyzer for the measurement of local state of polarization (SOP) in single mode fibers.

In a single mode optical fiber (SM) two orthogonal modes can spread along the fiber. Under ideal propagation conditions (cylindrical symmetry of the fiber, no outside physical field influence) no coupling between these modes does appear. Under real conditions the degeneration of modes takes place and the initially in one mode propagating energy is divided into two allowed orthogonal modes. This polarization phenomenon can be used for the description of the properties of optical route. If the mechanism of the change of SOP due to the influence of mechanical, magnetic, temperature or any other physical field is known, the PO–OTDR method can become a strong sensoric tool.

The principle of PO-OTDR is shown in the Fig. 1. As it was stated in the beginning of the paragraph the main difference between the traditional OTDR and PO-

OTDR consists in the additional monitoring of the SOP. That requires the use of an analyzer and polarizer. The optical impulse with the defined state of polarization is coupled through a splitter into the optical fiber. The backscattered signal is guided through the analyzer on the polarization independent photo detector. If a SM fiber with given polarization properties along its axis is considered, then the changes of SOP of the light signal caused by the influence of the external physical field can be directly determined.

The specified analyzer orientation angle θ_P (Fig. 1) during the measurement provides the information necessary for the specification of the measured local state of polarization,

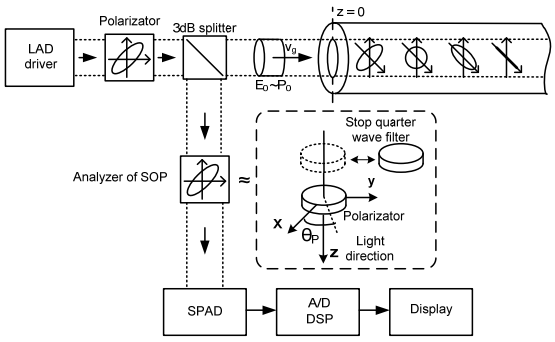

Fig. 1: Principle of PO – OTDR.

that is formulated in [2], [3], [4]. The main goal is to obtain the magnitude and the direction of the local birefringence vector β given by equation (1).

$$\vec{\beta} = \vec{\beta}_L + \vec{\beta}_C \,. \tag{1}$$

Where β_L is the magnitude of linear birefringence in untwisted fiber and β_C is circular birefringence which can be caused for instance by longitudinal magnetic field [5]. Linear birefringence is mostly caused by transverse mechanical load. The core of optical fiber is thus deformed into elliptical shape. The birefringence $\Delta\beta$ induced by the stress is represented by the expression:

$$\Delta\beta = \left|\beta_S - \beta_F\right| = \frac{\omega}{c}\Delta n_{eff} \,. \tag{2}$$

Where β_S, β_F are propagation constants for slow and fast mode and the Δn_{eff} is the effective differential index of refraction. Evolution of the SOP in OF is presented in the Fig. 2.

3. OTDR Based on Photon Counting

One of the unconventional approaches to OTDR is the "Photon Counting OTDR" (PC-OTDR) based on the application of the photon counting method [1]. PC-OTDR utilises the Poisson statistics of backscattered ultra low level optical power. The simplified diagram of the signal processing in PC–OTDR is shown in Fig. 3. In contrast with the classic OTDR it dominantly uses the digital signal processing.

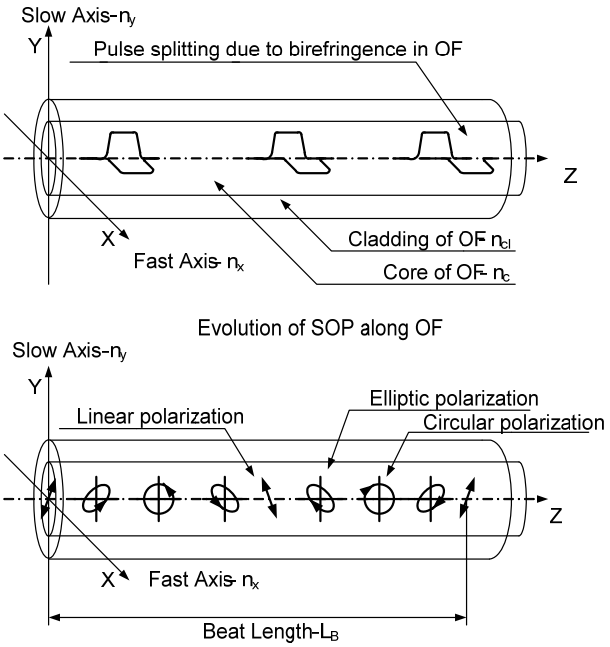

Fig. 2: Degradation of optical signal inside the optical fiber due to birefringence changes and the SOP evolution.

The optical source generates a test impulse which is launched through 3 dB optical coupler into the optical fiber. Backscattered photons from the fiber are detected by a very sensitive detector based on the single photon avalanche diode (SPAD). The result of the measurement is a PC-OTDR histogram. As it implies from the Poisson's statistics under specific conditions the measured values accumulated in the histogram are directly proportional to the backscattered power [2].

Let us consider the initial point of the time axis is coupled to the moment of the impulse launching. The creation of the histogram is then based on the repeated measurement of the time interval between the launching of the impulse and detecting of the first back scattered photon. The required signal noise ratio (SNR) is then achieved by sufficient number of repeated measurements. This phenomenon is common for all modified OTDR methods.

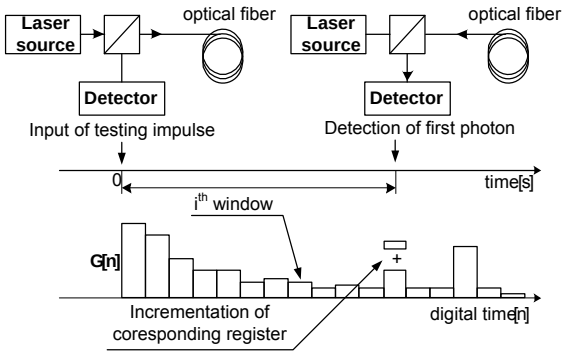

Fig. 3: The principle of PC-OTDR histogram forming [1].

4. The Elasto-Optical Phenomenon

As it was mentioned in chapter 2 any mechanical stresses applied to the optical fiber cause a reaction – dimension deformation and change of optical properties in a the fiber. The fundamental knowledge of such a phenomenon was given by stress-optic law given by Maxwell [7].

$$\begin{aligned} n_1 &= n_0 + C_1\sigma_{xx} + C_2(\sigma_{yy} - \sigma_{zz}) \\ n_2 &= n_0 + C_1\sigma_{yy} + C_2(\sigma_{zz} - \sigma_{xx}) \\ n_3 &= n_0 + C_1\sigma_{zz} + C_2(\sigma_{xx} - \sigma_{yy}) \end{aligned} . \quad (3)$$

Material properties are given by C_1 and C_2, where n_1, n_2 and n_3 represent the refractive index of the stressed material, n_0 of the unstressed one. The main stressesses in the space are represented by σ_{xx}, σ_{yy}, σ_{zz}. Equations (3) can be simplified to the form:

$$\begin{aligned} n_1 - n_2 &= C(\sigma_{xx} - \sigma_{yy}) \\ n_2 - n_3 &= C(\sigma_{yy} - \sigma_{zz}) \\ n_3 - n_1 &= C(\sigma_{zz} - \sigma_{xx}) \end{aligned} . \quad (4)$$

Where C is the photo-elastic constant defined as $C = C_1\text{-}C_2$. These equations represent the general case of the elasto-optical phenomenon in space.

For deeper analysis of the elasto-optical phenomenon in an optical fiber a simple model of lateral load on cylindrical fiber structure was simulated. The full field analytical solutions for distributed compressions could be found in [5], [6]. For more simple solution only the core of the fiber was considered. In the first analysis the fiber was subjected to the compression on two opposite sides. The geometric configuration of this problem is shown in Fig. 4.

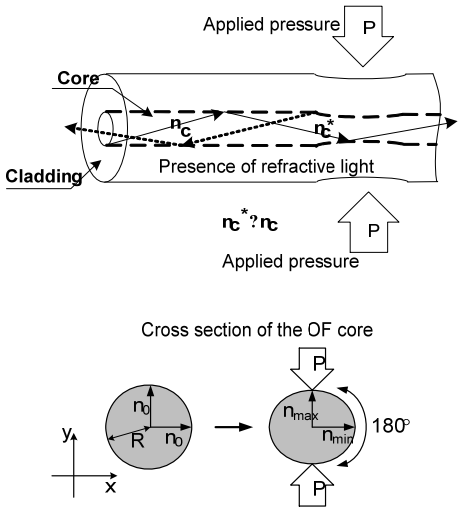

Fig. 4: The lateral stress loading on fiber core.

This situation can be described by Hertz solution for the stress distribution in the disk under diametrical compression.

In this solution the considered assumptions are appropriate for a high Young's modulus material [7] like silica fiber. The equations (5) and (6) for Hertz approximation are appropriate for plane strain description.

$$\sigma_{xx} = \frac{-2P}{N\pi}\left(\frac{x^2(R+y)}{\beta_2^4} + \frac{x^2(R-y)}{\beta_1^4} - \frac{1}{2R}\right), \quad (5)$$

$$\sigma_{YY} = \frac{-2P}{N\pi}\left(\frac{(R+y)^3}{\beta_2^4} + \frac{(R-y)^3}{\beta_1^4} - \frac{1}{2R}\right). \quad (6)$$

Where the lateral load is represented by P in load per thickness N. R is the geometrical radius of the fiber core. The β_1, β_2 are given by equation (7).

$$\beta_1^2 = x^2 + (R-y)^2, \beta_2^2 = x^2 + (R+y)^2 . \quad (7)$$

Another more precise model was given by Hondros equations. It's a solution for full field stresses but it has a series solution in polar coordinates which could be more challenging for simulation. The Hondros equations in [5] are expressed as follows:

$$\sigma_r = -\frac{2p}{\pi}\left\{\alpha + \sum_{n=1}^{n=\infty}\left[1-\left(1-\frac{1}{n}\right)\rho^2\right]\rho^{2n-2}\gamma\right\}, \quad (8)$$

$$\sigma_\theta = -\frac{2p}{\pi}\left\{\alpha - \sum_{n=1}^{n=\infty}\left[1-\left(1+\frac{1}{n}\right)\rho^2\right]\rho^{2n-2}\gamma\right\}, \quad (9)$$

$$\tau_{r,\theta} = \frac{2p}{\pi}\left\{\sum_{n=1}^{n=\infty}\left[1-\rho^2\right]\rho^{2n-2}\sin 2n\alpha \sin 2n\theta\right\}, \quad (10)$$

where γ is defined as

$$\gamma = \sin 2n\alpha \cdot \cos 2n\theta . \quad (11)$$

p is the applied pressure and α is the angle by loaded section of the rim. The ρ is the expression for r/R where R is disk radius. The maximum stress is coincidental to the y axis where the load is applied. That stress could be obtained by

$$\tau_{\max} = \left(\frac{P}{\pi r N}\right)\frac{1-\rho^2}{\rho^4 + 1 - 2\rho^2\cos 2\theta}. \qquad (12)$$

Using an approach like Hertz or Hondros the map of constant stress distribution in cross region of the fiber can be calculated. This stress field distribution is combined through the elasto-optic effect with the local change of refraction index. In [7] the photoelasticity is described by:

$$\Delta n_{eff\,x}(x,y,z) = -\frac{(n_{eff,0})^3}{2E}\times\left\{\begin{array}{l}(p_{11}-2\nu p_{12})\sigma_x(z,y,z)+\\ [(1-\nu)p_{12}-\nu p_{11}]\times\\ [\sigma_y(x,y,z)+\sigma_z(x,y,z)]\end{array}\right\}, \qquad (13)$$

$$\Delta n_{eff\,y}(x,y,z) = -\frac{(n_{eff,0})^3}{2E}\times\left\{\begin{array}{l}(p_{11}-2\nu p_{12})\sigma_y(z,y,z)+\\ [(1-\nu)p_{12}-\nu p_{11}]\times\\ [\sigma_x(x,y,z)+\sigma_z(x,y,z)]\end{array}\right\}, \qquad (14)$$

where n_{eff} is the effective index of refraction, E is the Young's modulus, ν is the Poisson's ratio and p_{11}, p_{12} are photoelastic constants obtained from [7].

4.1 Simulation Results

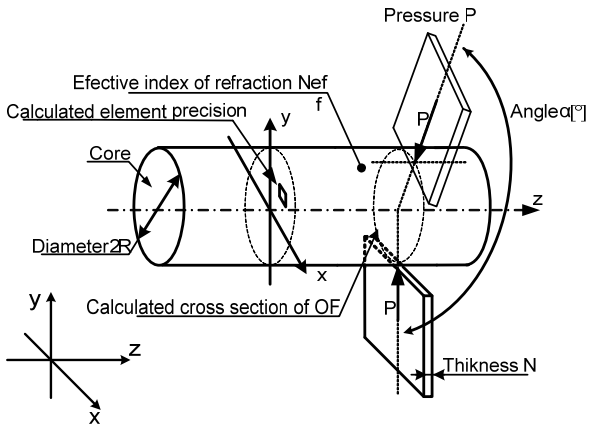

Fig. 5: Model of optical fiber sensor.

Taking into account equations (5), (6), (7) and the relation of stress to the index of refraction (13), (14) the elasto-optic phenomenon was modeled in MATLAB according to model on Fig. 5. Using the following input values:

E_{fiber} = 50 GPa
F = 10N
n_{eff} = 1,47
ν = 0,29
p_{11} = 0,121
p_{12} = 0,270

Figures 6 and 7 show graphically the effect of the lateral loading on the stress distribution in the fiber core as it results from the simulations in MATLAB.

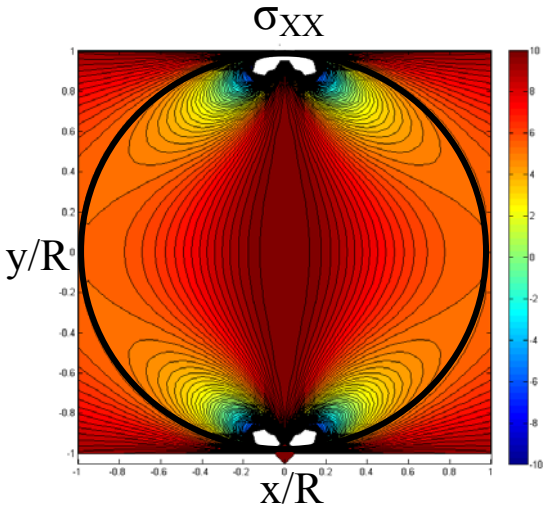

Fig. 6: Stress distribution σ_{xx} in fiber core cross section with lateral loading.

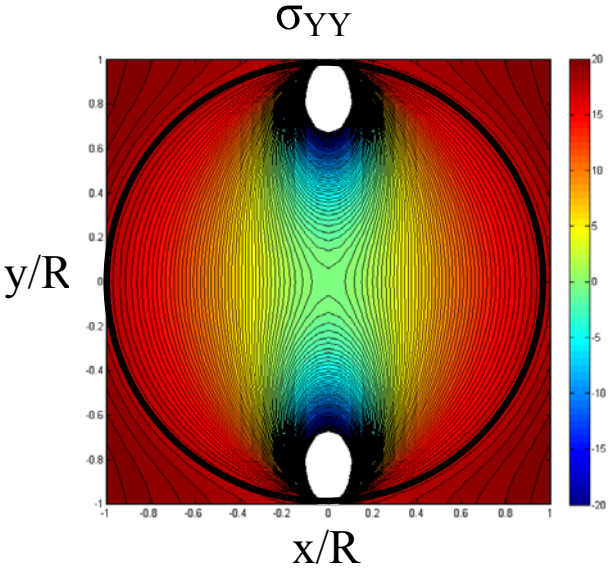

Fig. 7: Stress distribution σ_{yy} in fiber core cross section with lateral loading.

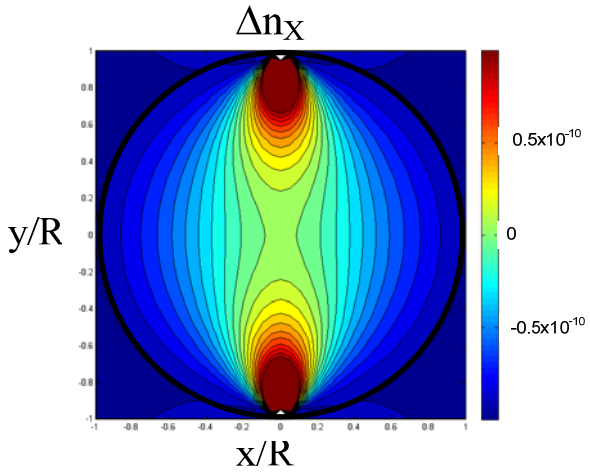

Fig. 8: Difference of the effective index of refraction Δn_X in the fiber core cross section under the loading.

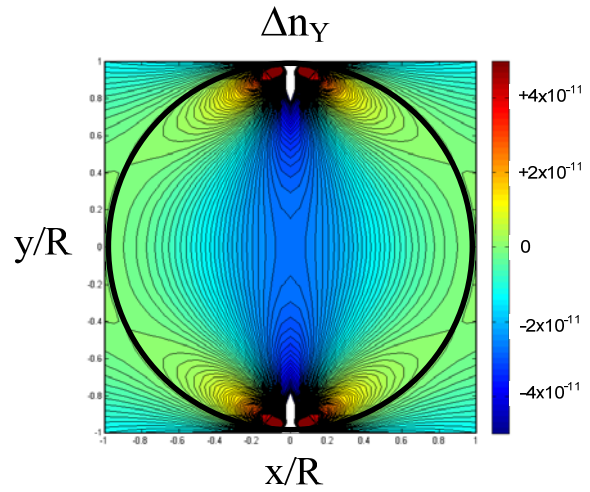

Fig. 9: Difference of the effective index of refraction Δn_Y in fiber core cross section under the loading.

The places of applied stress can be clearly seen from the simulation although the area of the pressure application is very small. The equipotent contours with higher amplitude of the pressure are clearly located along the y axis. Due to the pressure field in the atomic structure of fiber continuum, the index of refraction inside the core was changed up to 10^{-10}, which could be seen in the Fig. 9.

The fluctuations in the index of refraction are the reason why the pressure fields on fibers can cause additional linear birefringence. If the polarization properties of the fiber are known before its exposure to the stress that is perpendicular to the fiber axis, polarimetric sensor with distributed parameters can be obtained.

To obtain more precise model of OF a cylindrical symmetric structure of silica material was modeled in ANSYS Multiphysics program. The structure consists of two cylindric areas consisting of different materials. Inner core with the diameter of 10 μm and cladding of 120 μm. To simulate the difference of "optical density" between core and cladding the Young modulus parameter was set to 55 GPa for the core and to 50 GPa for cladding. Each part was meshed for finite numerical analysis. On four model segments (nodes) the force of 100 μN was applied.

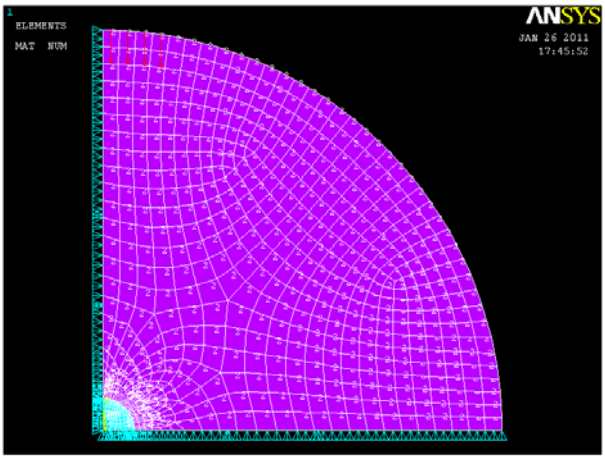

Fig. 10: Symmetric model of OF realized in ANSYS.

The results were displayed as an expanded periodic ¼ dihedral model to obtain result which can be compared to Fig. 6 and Fig. 7.

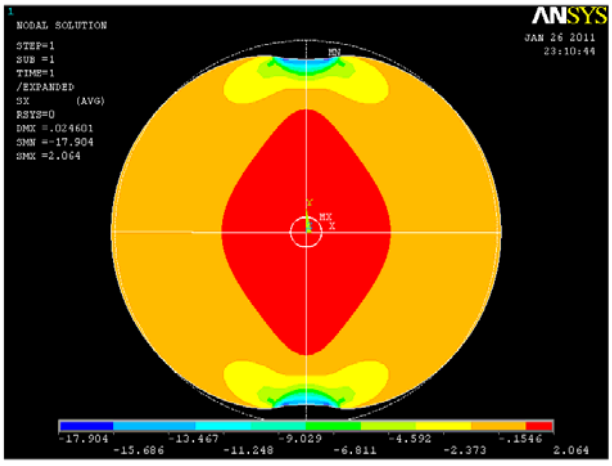

Fig. 11: Stress distribution σ_{xx} in cylindrical fiber cross section structure with lateral loading.

The results obtained from ANSYS clearly show that the previous simulations in MATLAB were a good approximation of the pressure distribution σ_{XX}, σ_{YY}. ANSYS simulations have also shown that the cylindrical structure becomes more elliptic and the pressure inside the fiber core will change. Due to these changes additional birefringence will affect the SOP and the periodicity of the beat length will contain retardation. PO

OTDR measuring method provides a tremendous possibility to detect such effects and to use them in sensor applications.

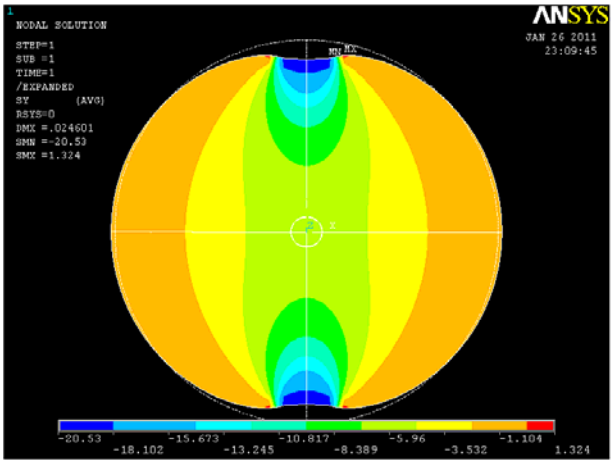

Fig. 12: The stress distribution σ_{yy} in the cylindrical fiber cross section structure with lateral loading.

5. The Concatenated Fiber Model

For an easy understanding of the birefringence distribution along an OF the model is introduced as shown in Fig. 7. The axis of each birefringent fiber segment is randomly rotated [8].

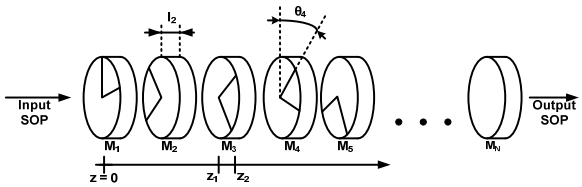

Fig. 13: The fiber model with random birefringence.

Each of the fiber segments is described by the appropriate Jones matrix J_i as it is shown in the Fig. 13. The Jones matrix, describing the total birefringence experienced by the light propagating from the input end of the fiber to the end of the i-th element, is given by the relation product of individual matrices [9].

$$J_{e(i-1)} = J_{(i-1)} J_{(i-2)} \ldots\ldots J_{(1)} . \qquad (15)$$

The $M_{e(i-1)}$ is the polarization matrix of the preceding fiber elements. If we couple the testing impulse with the given SOP signed as I_{in} the output SOP is then given by

$$I_{OUT} = J_{e(i-1)}{}^{2} I_{in} . \qquad (16)$$

The Jones vector is suitable for those task solutions. Jones vector is a column matrix of two elements, which describes the beam polarization in the specific place along the fiber axis.

$$J_i = \begin{bmatrix} E_x \\ E_y \end{bmatrix} = \begin{bmatrix} A_x e^{j(\varphi_x + 2\pi\nu t)} \\ A_y e^{j(\varphi_y + 2\pi\nu t)} \end{bmatrix}, \qquad (17)$$

Where E_x, E_y are the vector components at specific moment t. A_x and A_y are the maximum amplitudes and φ_x, φ_y are the phase shifts at the time t = 0.

The other approach suitable for the description of the SOP is also the use of 4- component Stokes vector [9]. The principle of this approach is shown in the Fig. 1. (analyzer block). The transmission axis of the polarizer and the x axis of the fixed coordinate system contain the angle θ_P. Fast axis of the stop quarter filter (SQF) is collinear with the x axis. Then one has to measure the light intensity $I(\theta,\delta)$ where δ can be $\pi/2$ or 0. It depends on the situation if the SQF is applied or not. Then for the Stokes vector holds the following relation:

$$\begin{bmatrix} S_0 \\ S_1 \\ S_2 \\ S_3 \end{bmatrix} = \begin{bmatrix} I(0,0) + I\left(\frac{\pi}{2},0\right) \\ I(0,0) - I\left(\frac{\pi}{2},0\right) \\ I\left(\frac{\pi}{4},0\right) - I\left(\frac{3\pi}{4},0\right) \\ I\left(\frac{\pi}{4},\frac{\pi}{2}\right) + I\left(\frac{3\pi}{4},\frac{\pi}{4}\right) \end{bmatrix}. \qquad (18)$$

6. PC OTDR Results

The PO OTDR measurements where done in our laboratory on our experimental PO OTDR reflectometer based on photon counting. The tested fiber was SMF 28 Corning with the beat length 28 m and n_c = 1,47. The optical input testing impulse was 5 ns wide. The results from the first 500 meters are shown in the Fig. 14, Fig. 15, Fig. 16.

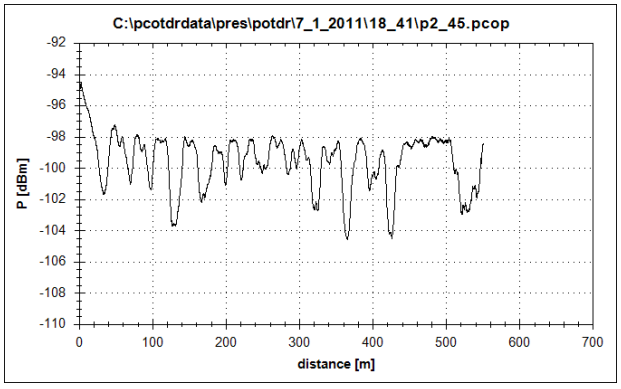

Fig. 14: PC OTDR reflectogram with 45° angle of the analyzer.

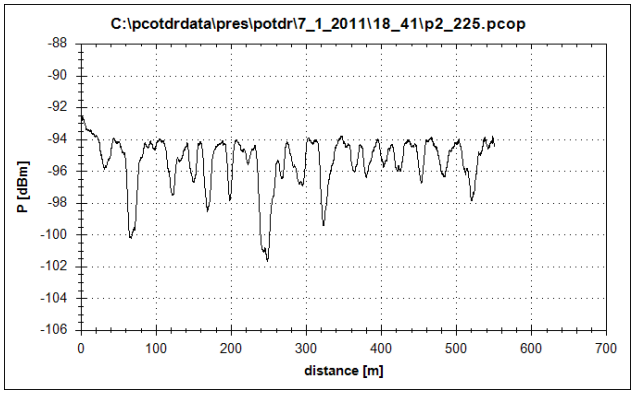

Fig. 15: PC OTDR reflectogram with 22°5′ angle of the analyzer.

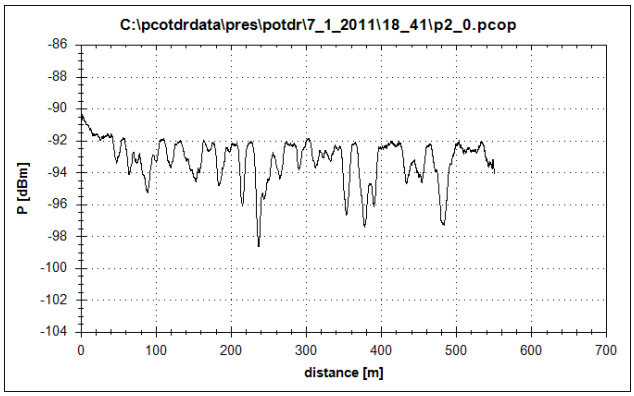

Fig. 16: PC OTDR reflectogram with 0° angle of the analyzer.

From the results it can be seen that some sectional periodicity in the measured signal is obtained. This is in agreement with the theory [9]. Further research and better signal processing methods are needed to obtain birefringency data and will be the subject for our next work.

7. Conclusion

In the first part of the paper the results of the numerical simulation of the elasto-optic effect in the standard cylindrically symmetrical optical fiber are brought. The main result consists in the evaluation of the space changes of the local refraction index in the optical fiber core under the defined mechanical side load. These changes imply the occurrence of induced local birefringence in optical fiber. The exact investigation of the relation between the sensed physical quantity and induced birefringence is the crucial point for the construction of smart fiber optic sensors with distributed parameters.

The application and may be further elaboration of the presented approach can significantly contribute to the contemporary fiber sensing applications with distributed parameters. For the better and more precise measurement the more sophisticated models for the interaction between the external fields of influence and the optical fiber are needed.

Acknowledgments

This work was done as a part of the solution of the VEGA projects No. VEGA 9337/06 and VEGA 1/0617/5.

References

[1] BARNOSKI, M. K.; JENSEN, S. M. Fiber waveguides : A novel technique for investigation of attenuation characteristics. In: *Applied Optics*. 1976, vol. 15, no. 9, pp. 2112-2115. ISSN 2155-3165.

[2] ORLANDINI, A.; VINCETTI, L. Jones transfer matrix for polarization mode dispersion fibers. In: *Lasers and Electro-Optics Society 2000 Annual Meeting*. LEOS 2000. 13th Annual Meeting. IEEE. 2000, vol. 1, pp. 218-219. ISBN 0-7803-5947-X.

[3] LUNEBURG, E.; CLOUDE, R. S. On the proper polarimetric scattering matrix formulation of the forward propagation versus backscattering radar systems description. In: *Geoscience and Remote Sensing, 1997. IGARSS '97. Remote Sensing - A Scientific Vision for Sustainable Development., IEEE International.* 1997, vol. 4, pp. 1591-1593. ISBN 0-7803-3836-7.

[4] ORLANDINI, A.;VINCETTI, L. A simple and useful model for Jones matrix to evaluate higher order polarization-mode dispersion effects. In: *Photonics Technology Letters, IEEE*. 2000, vol. 13, no. 11, pp. 1041-1178. ISSN 1041-1135.

[5] HUNG, K.M., et al. Theoretical analysis and digital photoelastic measurement of circular disk subjected to partially distributed compressions. In: *Experimental mechanics*. 2003, vol. 43, no. 2, pp. 216-224. ISSN 0014-4851.

[6] MIGLIORE, A. R.; ZANOTTO, E. D. Fracture strength of glass analyzed by different testing procedures. In: *Glass technology*. 1996, vol. 37, no. 2, pp. 95-98.

[7] MASTRO, S. A. *Optomechanical behaviour of embedded fiber bragg grating strain sensors* [online]. 2005. Ph.D. thesis. DREXEL UNIVERSITY. Available at WWW: <http://dspace.library.drexel.edu/bitstream/1860/515/10/Mastro_Stephen.pdf>.

[8] PILINSKY, S. Z; ŠIPUŠ, Z.; ŠUMICHRAST, Ľ. Modeling of optical link using finite - difference method. In: *International Conference on Telecommunications, ConTEL* 2003. Proceedings of the 7th. 2003, vol. 2, pp. 383-388. ISBN 953-184-052-0.

[9] JASENEK, J. The use of polarization optical time domain reflectometry for the birefringence distribution measurement along the SM optical fiber. In: *17th International Conference Radioelektronika 2007* [online]. Available at WWW: <http://www.urel.feec.vutbr.cz/ra2007/archive/ra2002/pdf/124.pdf>. ISBN 1-4244-0821-0.

[10] HLAVÁČ, M.; JASENEK, J.; ČERVEŇOVÁ, J. Distributed fiber optic sensor for traffic monitoring. In: *Third European Workshop on Optical Fiber Sensors*. 2007, vol. 6619, 661939 (2007). ISBN 978-0819467614.

About Authors

Branislav KORENKO was born in 1985 in Poprad, Slovakia. He received his M.Sc. degree in the study field Radioelectronics from the Slovak University of Technology, Bratislava in 2009. His work is focused

mainly on the analysis and the design of high speed electronic circuits for OTDR signal processing with the applications in the construction of the optical fiber sensors with distributed parameters. At present he is working on his Ph.D. studies.

Jozefa CERVENOVA was born in 1958 in Bratislava, graduated from the Faculty of Electrical Engineering and Information Technology of the Slovak University of Technology in Bratislava in 1982 in the study field Solid State Physics. She completed her Ph.D. studies in 1993 in the field of Electromagnetic Theory. She took part in the solution of several VEGA scientific research projects oriented to optical fiber technology. Her current research interests concern mainly the testing methods of optical fiber systems and components.

Jozef JASENEK was born in 1947, in Bobrov (Slovakia), graduated from the Faculty of Electrical Engineering and Information Technology of the Slovak University of Technology Bratislava in 1971, in he study field Solid State Physics. Since 2004 he is a Full Professor in Electromagnetic theory. Currently his professional interests concern mainly the theory of linear and nonlinear optical waveguides and the development of experimental methods for testing of optical waveguides and optical fiber components. Especially he is involved in analysis and implementation of optical reflectometric methods (OTDR and its modifications). He has lead several scientific projects and published more than 40 scientific papers and two monographs.

Marek HLAVAC was born in Malacky, Slovakia in 1979. He received his M.Sc. degree in Electronics from the Slovak University of Technology, Bratislava, in 2005. His research activity is focused on the fiber optic sensors, photon counting measurement method and polarization sensitive measurements in fiber optics. Currently he is working on completion of his Ph.D. studies.